Electronic Supplementary Material (ESI) for ChemComm.

Supporting Information

Fluorescence sensing of nitrophenol explosives using two-dimensional organic-metal chalcogenides with fully covered functional groups

Yu Pan, [ab] Chengpeng Wang, [a] Zhihua Fu,[ab] Guang-E Wang *[ab] and Gang Xu *[ab]

[a] State Key Laboratory of Structural Chemistry, Fujian Institute of Research on the Structure of Matter, Chinese Academy of Sciences (CAS),
No. 155 Yangqiao Road West, Fuzhou, Fujian, 350002, P. R. China
[b] University of Chinese Academy of Sciences (UCAS),
No. 19A Yuquan Road, Beijing 100049, P. R. China

Corresponding author: Gang Xu
gxu@fjirsm.ac.cn

Experimentation

Characterization. The single crystal X-ray diffraction measurement was performed on a Rigaku SATURN70 CCD diffractometer using graphite-monochromated Mo-Kα radiation (λ = 0.71073 Å). Intensity data set was collected using an ω scan technique and corrected for *Lp* effects. The primitive structure was solved by the direct method using the Olexsys Olex2™ Version 1.2.10 package of crystallographic software. The difference Fourier maps based on these atomic positions yield the other nonhydrogen atoms. The final structure was refined using a full-matrix least-squares refinement on F^2. All nonhydrogen atoms were refined anisotropically. Hydrogen atoms on carbon and oxygen atoms were generated geometrically. However, it is definitely hard to collect great crystal data of compound **1** because 2D crystal structure tends to be polycrystalline. Crystallographic data for CdClHT is listed in Table S1. Therefore, the simulated and experimental powder X-ray diffraction (XRD) patterns of the microplates are indexed and mutually verified.

Powder X-ray diffraction (PXRD) of samples were recorded on a Rigaku Smartlab MiniFlex 600 X-ray diffractometer using Cu *K*α radiation (λ = 1.54178 Å) at 30 kV and 15 mA. The simulated PXRD pattern of $Cd_3Cl_2(HT)_4$ was derived from the Mercury Version 3.9 software. Scanning electron microscope (SEM, ZEISS-300) was operated at 5.0 kV. Transmission electron microscope (TEM) images were obtained on a JEOL-2010 transmission electron microscope at an acceleration voltage of 200 kV. Atomic force microscopy (AFM) measurements were performed using Bruker dimension ICON scanning probe microscope with Peakforce tapping mode. Fourier transform infrared spectroscopy (FTIR) spectra were recorded on a Bruker VERTEX70 FT-IR spectrometer (Germany) in 4000–600 cm^{-1} region using KBr pellets. Thermogravimetric analysis (TGA) of $Cd_3Cl_2(HT)_4$ was performed on a NETZSCH STA 449F3 analyzer under a stream of nitrogen of 20 mL min^{-1}. The samples were heated from 30 to 900 °C at a heating rate of 10 °C min^{-1}. Edinburgh FLS980 fluorescence spectrometer was used to characterize the solid-state photoluminescent property of compound **1** at room temperature, CIE chromaticity coordinates was calculated using the CIE calculator version 1.6 software.

Synthesis of $Cd_3Cl_2(HT)_4$. $2(CdCl_2)\cdot 5(H_2O)$, 4-Hydroxythiophenol and ethanol were received from Adamas-beta. They were directly used without further purification. $2(CdCl_2)\cdot 5(H_2O)$ (22.8 mg, 0.1 mmol) dispersed in deionized water (5ml) and 4-Hydroxythiophenol (70 μL) dispersed in methanol (5 mL) at first, mixed in a glass bottle, then, heated at 85℃ for 96 hours. Cool naturally to room temperature, white transparent plant crystals were obtained in 29.2 % yield. Elemental analysis reveals that **1** contains 31.74% C and 2.193% H, which is nearly consistent with the calculated values from the chemical formula: 31.71% C and 2.2% H.

Preparation of few layer nanosheets. 10 mg powder sample was dispersed in 50 mL ethanol. The dispersion was placed in in a sonic bath at power output of 200 W for 2 h with 200 W power, and then the power was adjusted to 320 W for 2 hours to obtain a uniform dispersion. A drop was randomly selected for scanning probe microscope observation, and the result showed that the thickness was ~5 nm.

Fluorescence quenching test. 5 mg few layer nanosheets sample was ultrasonically dispersed in

50 mL ethanol for 10 minutes, then stood for 12 h, and the upper evenly dispersed solution was taken for fluorescence test. Add 20 μL (1 mmol per liter) of the analyte solution each time and observe the change of fluorescence intensity.

Result and discussion

Table S1. Crystallographic data for CdClHT.

Empirical formula	$C_{12}H_{10}Cd_{1.5}ClO_2S_2$
Formula weight	454.1
T (K)	99.98(13)
Crystal system	monoclinic
Space group	$P2_1/c$
a (Å)	16.5869(7)
b (Å)	11.9546(5)
c (Å)	14.0741(7)
α (°)	90
β (°)	109.534
γ (°)	90
V (Å^3)	2630.1(2)
Z	8
ρ_{calc}g/cm^3	2.295
μ/mm^{-1}	16.537
F(000)	1764.3
Radiation	micro-focus metaljet (λ = 1.3405)
2Θ range for data collection/°	4.92 to 121.06
Index ranges	-21 ≤ h ≤ 21, -14 ≤ k ≤ 15, -9 ≤ l ≤ 18
Reflections collected	17147
Independent reflections	5813 [R_{int} = 0.0897, R_{sigma} = 0.0701]
Data/restraints/parameters	5813/0/338
Goodness-of-fit on F^2	2.157
Final R indexes [I>=2σ (I)]	R_1 = 0.1976, wR_2 = 0.4901
Final R indexes [all data]	R_1 = 0.2100, wR_2 = 0.4979

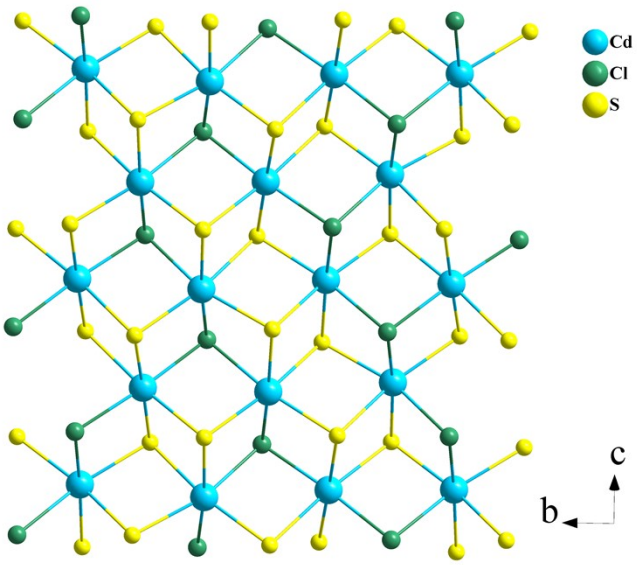

Fig. S1 2D $\{CdClS\}_n$ layer viewed along the *a* aixs.

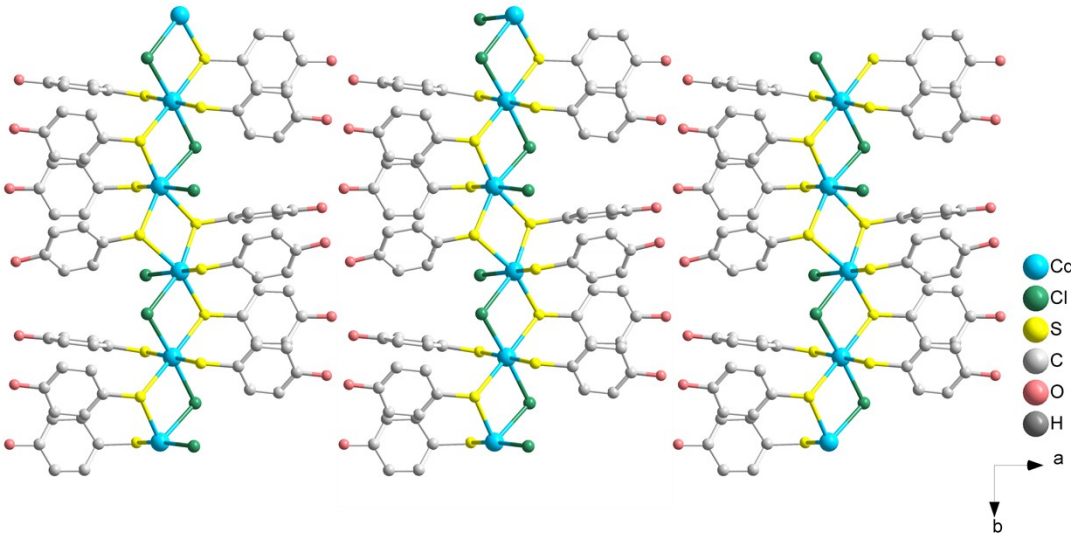

Fig. S2 Packing structure of CdClHT perpendicular to *c* direction.

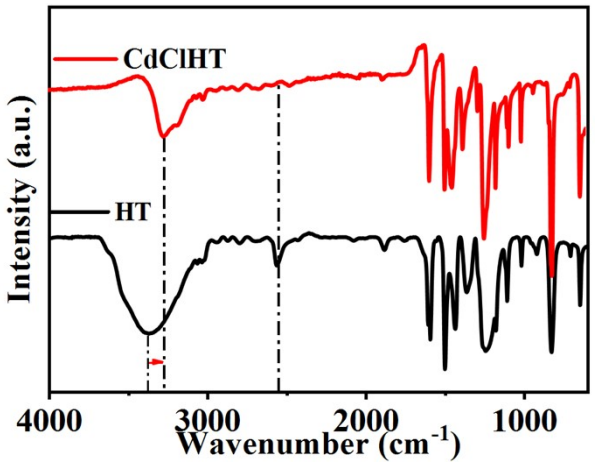

Fig. S3 FTIR spectrum of HT and CdClHT.

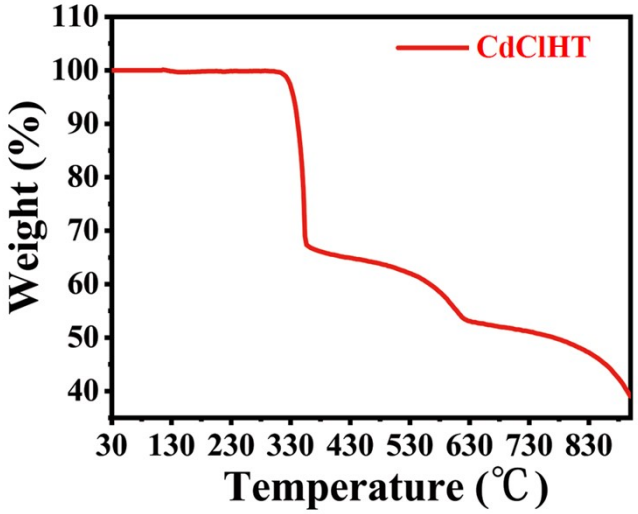

Fig. S4 TG curve of **1**. Compound 1 shows a weight loss of around 35 % between 300 and 400 °C which can be assigned to decomposition of the arylthiolate ligand and subsequent formation of Cd(II) sulfide and Cd halides. Meanwhile, part of O was captured by Cd to form Cd oxides, Similar thermal transformations have been reported for $[Cu_3X(HT)_2]_n$ (X=Cl, Br, and I), with decomposition temperatures between 250 and 350 °C.[1] At the range of 550-650 °C, a weight loss can be mainly assigned to extra S which failed to form CdS. At the third step, the weight loss can mainly assigned to the decomposition of Cd halides.

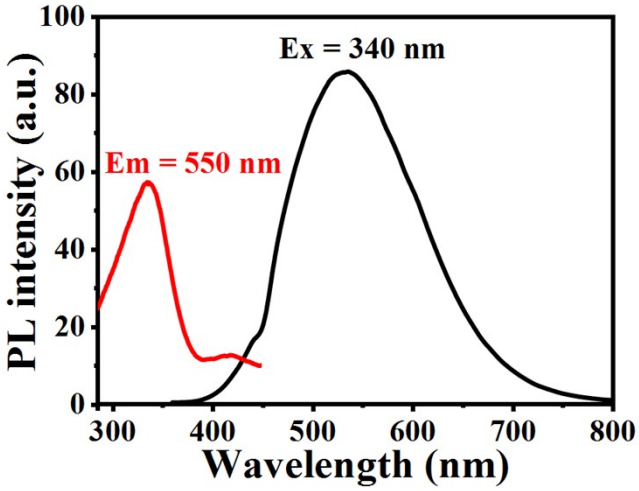

Fig. S5 The PL spectrum of the powder sample.

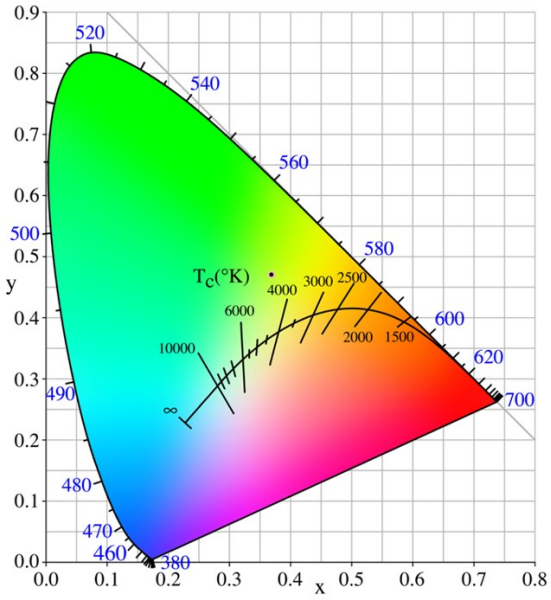

Fig. S6 CIE chromaticity coordinates of **1**.

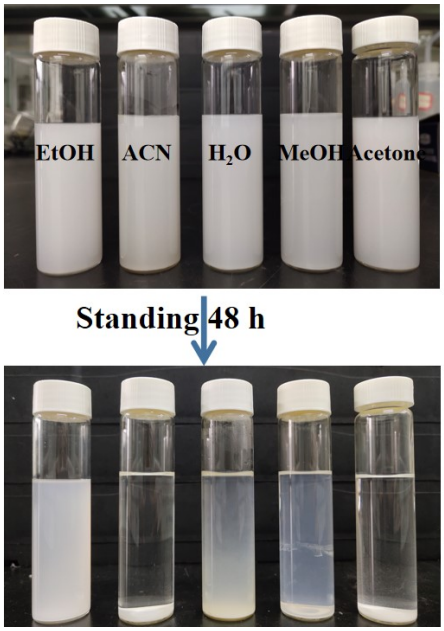

Fig. S7 Dispersion state of **1** ultrasonic dispersion in different solvents and stand for 48 h.

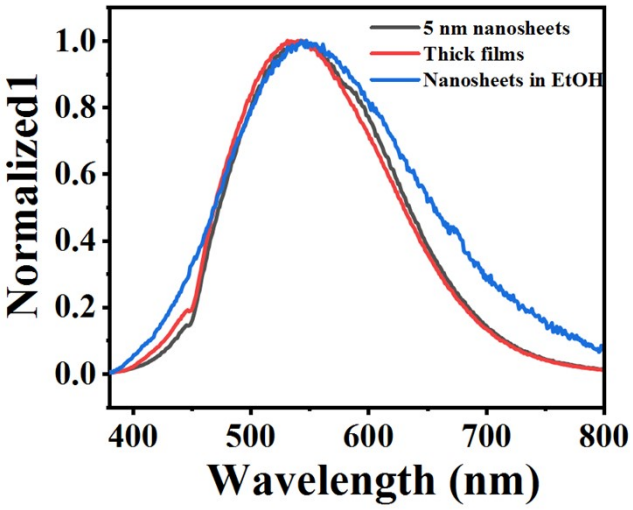

Fig. S8 Emission spectra of **1** excitation at 340 nm.

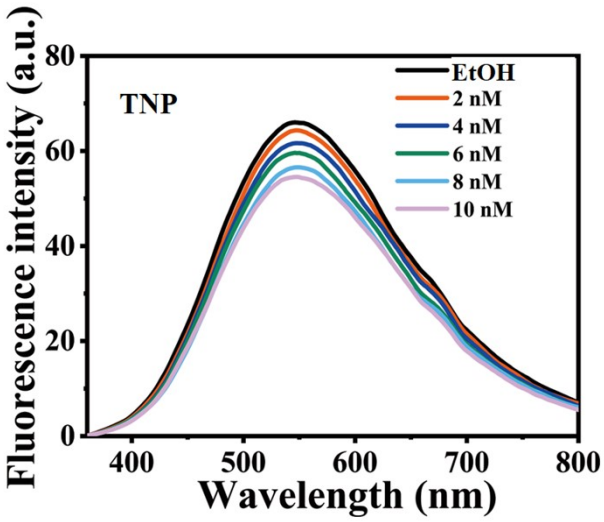

Fig. S9 Emission spectra of **1** dispersed in EtOH upon incremental addition of TNP solution (2-10 nM) in EtOH.

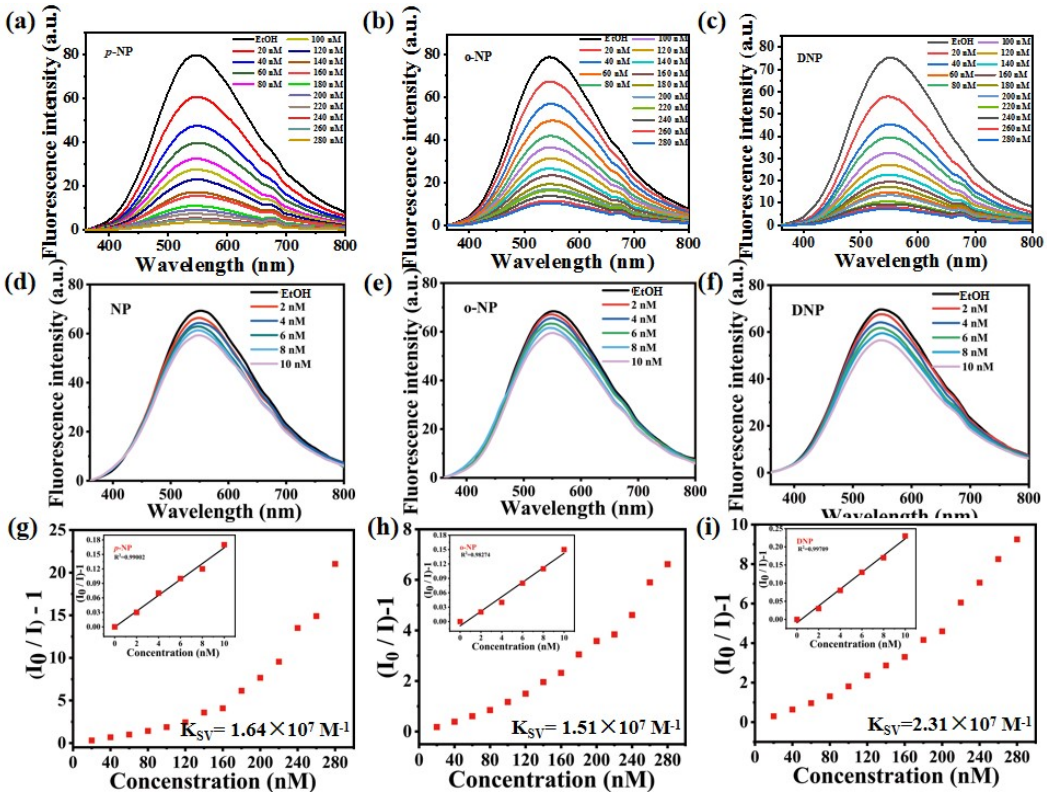

Fig. S10 Emission spectra of **1** dispersed in EtOH upon incremental addition of (a) p-NP, (b) o-NP, (c) DNP solution (20-280 nM) and (d) p-NP, (e) o-NP, (f) DNP solution (2-10 nM) in EtOH. SV plots of (g) p-NP, (h) o-NP, (i) DNP.

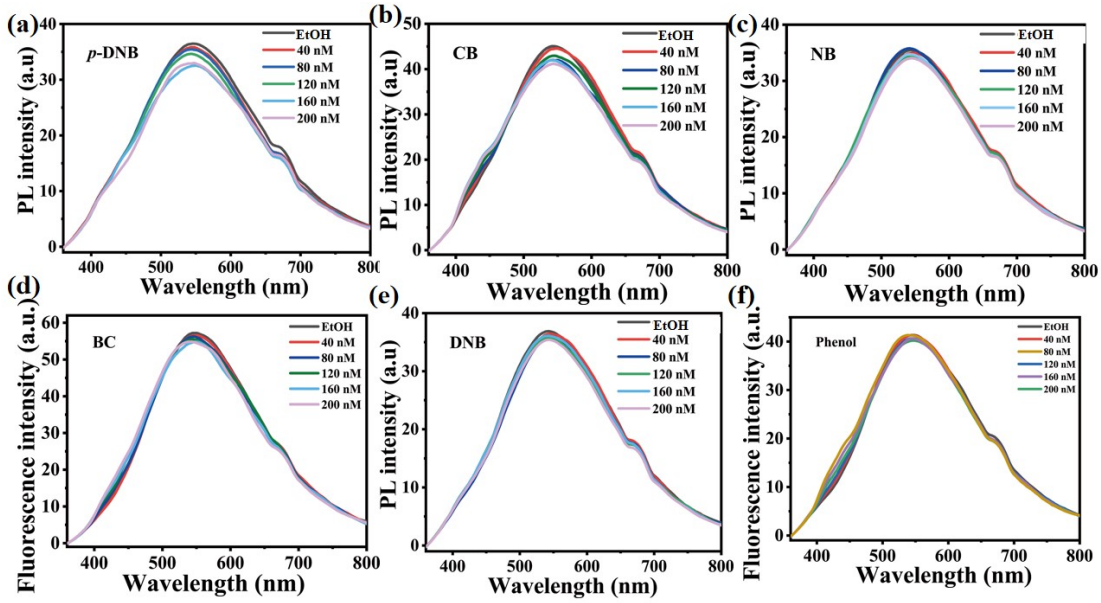

Fig. S11 Emission spectra of **1** dispersed in EtOH upon incremental addition of (a) p-DNB, (b) CB, (c) NB (d) BC, (e) m-DNB, (f) Phenol solution (40-200 nM) in EtOH.

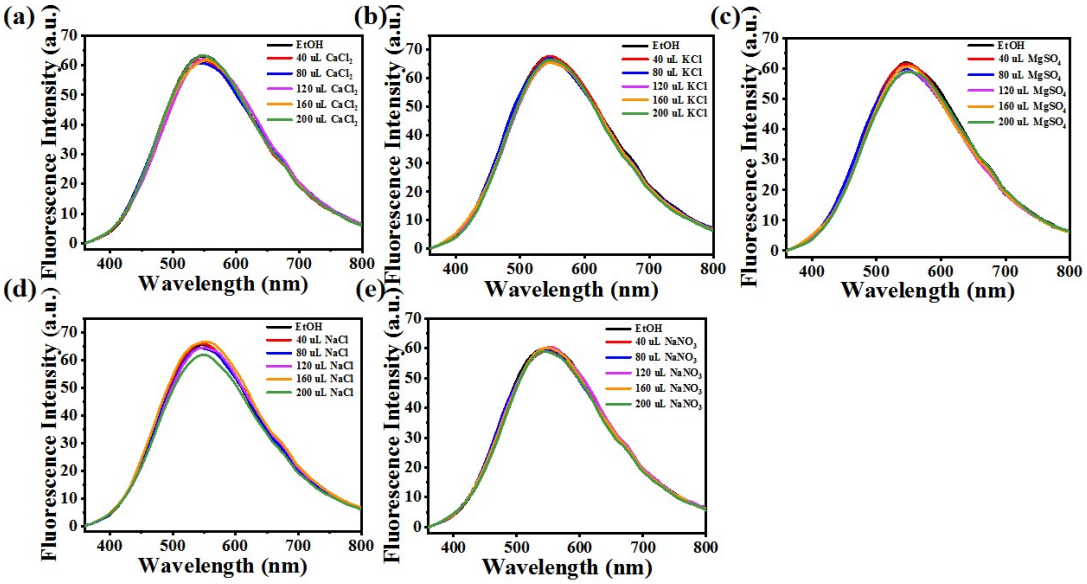

Fig. S12 Emission spectra of **1** dispersed in EtOH upon incremental addition of (a) $CaCl_2$, (b) KCl, (c) $MgSO_4$ (d) NaCl, (e) $NaNO_3$ (40-200 nM) in EtOH.

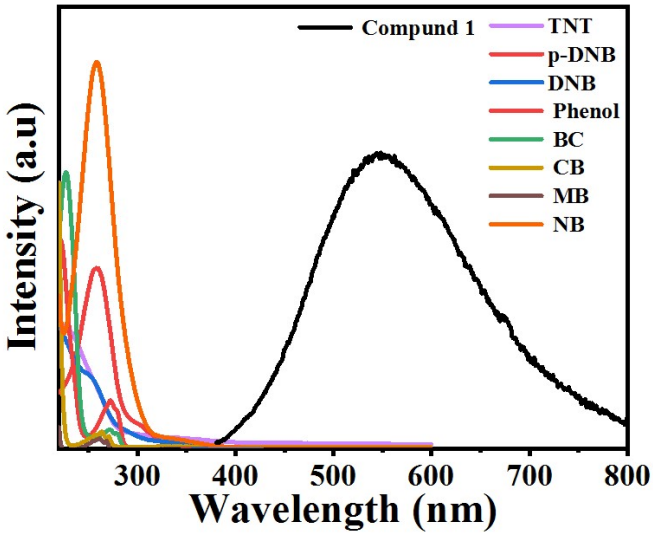

Fig. S13 Spectral overlap between the absorption spectra of analytes and the emission spectrum of **1** in EtOH.

Table S1. The reported quenching constant of the TNP with 2D CPs including LMOFs and LCOF.

Material		Detecting system	K_{SV} (M^{-1})	LOD (μM)	Reference
CUST-506 (Eu-MOF)	MOF	water	3.64×10^4	0.175	2
$[La(H_2O)_4(HL)]\cdot H_2O$	MOF	water	4.61×10^4	4.13	3
$[Zn(3\text{-cptpy})Cl]_n$	CP	DMF	3.86×10^4	2.45	4
$[Cd(3\text{-cptpy})_2]_n$	CP	DMF	3.26×10^4	2.08	5
$\{[Cd(suc)(4\text{-nvp})_2]\cdot 2H_2O\}_n$	CP	ACN	5.13×10^5	0.91	6
Tb-CP	CP	water	3.81×10^4	0.05	7
$\{[Zn(2,5\text{-tdc})(3\text{-abit})]\cdot H_2O\}_n$	MOF	DMF	4.71×10^4	1.46	8
TfpBDH-CONs	COF	IPA	2.6×10^4	54*	9
$Zn_2(H_2L)_2(Bpy)_2(H_2O)_3\cdot H_2O$	MOF	Water	1.36×10^4	0.49	10
DBQP	CMP	Acetone	9.02×10^4	3.33×10^{-12}	11
DBQN	CMP	Acetone	1.79×10^4	2.48×10^{-7}	11
$[(Pr_2(TATMA)_2)\cdot 4DMF\cdot 4H_2O]_n$	MOF	DMF	1.6×10^4	0.6 ppm*	12
$[Pb(L\text{-}F)Cl]_n$	CP	DMF	1.39×10^4	14.1	13
$[Cd(5\text{-}BrIP)(TIB)]_n$	MOF	Water	2.68×10^4	0.27	14
$[Zn(\mu_2\text{-}1H\text{-}ade)(\mu_2\text{-}SO_4)]$	CP	Water	3.14×10^4	4×10^{-4}	15
Yb-MOFs	MOF	$K_2S_2O_8$ system	—	0.0831	16
Y-MOF:Eu	MOF	ACN	3.21×10^4	4	17
Y-MOF:Tb	MOF	ACN	3.19×10^4	6.5	17
$[Zn(pzt)_2]_n$	CP	EtOH	2.45×10^4	0.4	18
[Zn(PAM)(en)]	CP	DMSO	—	2.59	19
$[Mg(DMF)_4Ag_2(SCN)_4]_n$	CP	DMF	1.98×10^4	0.794	20
$\{[Zn(L)(H_2O)_2]\cdot H_2O\}_n$	CP	Water	9.77×10^4	0.63	21

$\{[Cd(L)(H_2O)_2]\cdot H_2O\}_n$	CP	Water	8.52×10^4	0.75	21
$\{Cd(INA)(pytpy)(OH)\cdot 2H_2O\}_n$	CP	DMF	4.3×10^4	2.41	22
$[Cd_3(NTB)_2(DMA)_3]\cdot 2DMA$	MOF	DMA	2.0×10^4	1 ppm*	23
$\{[Cu^I_2(ttpa)_2][Cu^{II}(bptc)]\cdot 3H_2O\cdot DMF\}_n$	MOF	EtOH	6.65×10^4	0.22	24
$\{[Cu(L)(I)]\cdot(DMF)\cdot H_2O\}_n$	MOF	MeCN	1.51×10^5	215 ppb	25
$\{Zn_2(tpbn)(2,6\text{-}NDC)_2\}_n$	MOF	DMF:H_2O (4:1)	2.89×10^4	0.7 ppm	26
$\{Zn_2(tphn)(2,6\text{-}NDC)_2\cdot 4H_2O\}_n$	MOF	EtOH:water (4:1)	2.2×10^4	1.6 ppm	16
Zn-NDC-MI	CP	Water	4.32×10^4	0.058*	27
$[Zn(HL)\cdot 1.5H_2O]$	CP	Water	1.65×10^4	1.23 ppm	28
$\{[Dy(\mu_2\text{-}FcDCA)_{1.5}(MeOH)(H_2O)]\cdot 0.5H_2O\}_n$	MOF	Water	8.55×10^4	0.71	29
$[Zn(ttb)(bdc)_{0.5}]_n$	MOF	Water	1.56×10^5	0.04	30
DTZ-COF	COF	THF	8.71×10^4	0.357	31
$[Cd_2(H_2L)_2(2,2'\text{-bipy})_2]$	CP	DMF	2.85×10^3	0.86 ppm	32
$[Cd(L)_{0.5}(phen)\cdot 0.5H_2O]$	CP	DMF	2.25×10^3	0.94 ppm	32
$[CuI(BPDPE)]_n$	MOF	MeCN	1.5×10^4	1.09	33
$[L_4Cd_3(H_2O)_2]_n$	MOF	Water	6.6×10^4	0.119	34
$\{Cd(L_2\}_n$	CP	Water	6.87×10^4	0.089	35
$\{[WS_4Cu_4I_4[Ni(PBPP)_2]]2DMF]\}_n$	MOF	Water	1.51×10^4	1.73	36
$[Eu_2(ppda)_2(npdc)(H_2O)]\cdot H_2O$	MOF	MeOH	3.44×10^5	2.97	37
CdClHT	CP	EtOH	2.16×10^7	0.002*	**This work**

*: Experimental LOD. Others are theoretical LOD.

Definitions of the abbreviations used for the compounds listed in table: CUST-506 = $[Eu(L\text{-}N_2)_2\cdot(L\text{-}Cl_4)_{1.5}\cdot H_2O]$ ($L\text{-}Cl_4$ = 2,3,5,6-tetrachloroterephthalic acid, $L\text{-}N_2$ = 1,10-phenanthroline);[2] $[La(H_2O)_4(HL)]\cdot H_2O$ (HL = azodioxybenzenetetracarboxylic acid);[3] $[Zn(3\text{-cptpy})Cl]_n$: 3-Hcptpy = 40-(4-carboxyphenyl)-3,2′:6′,3′′-terpyridine;[4] $[Cd(3\text{-cptpy})_2]_n$ = poly[μ[3-4-(3,2′:6′,3′′-terpyridin-4′-yl)benzoato]cadmium(II)];[5] $\{[Cd(suc)(4\text{-nvp})_2]\cdot 2H_2O\}_n$: ($H_2$suc = succinic acid and 4-nvp = 4-(1-naphthylvinyl)pyridine);[6] Tb-CP: L = 3-bis(3-carboxyphenyl) imidazolium;[7] $\{[Zn(2,5\text{-tdc})(3\text{-abit})]\cdot H_2O\}_n$: 2,5-tdc = 2,5-thiophenedicarboxylic acid, 3-abit = 4-amino-3,5-bis(imidazol-1-ylmethyl)-1,2,4-triazole);[8] TfpBDH-CONs: Tfp = 1,3,5- tris(4-formylphenyl)benzene, BDH = pyromellitic-N,N/-bisaminoimide and CON = Covalent Organic Nanosheets;[9] $Zn_2(H_2L)_2(Bpy)_2(H_2O)_3\cdot H_2O$: Bpy = 4,4′-bipyridine;[10] DBQP and DBQN: The benzoquinone-based conjugated microporous/mesoporous polymers were synthesized with tetrabromo-1,4-benzoquinone (TBrBQ) and 1,4-diethynylbenzene (DEB) by both solution polymerization (DBQP) and miniemulsion polymerization (DBQN);[11] $[(Pr_2(TATMA)_2)\cdot 4DMF\cdot 4H_2O]_n$: H_3TATMA = 4,4′,4′′-*s*-triazine-1,3,5-triyltri-maminobenzoate;[12] $[Pb(L\text{-}F)Cl]_n$: L-F = 5-fluoronicotinic acid;[13] $[Cd(5\text{-}BrIP)(TIB)]_n$: H_2BrIP = 5-Bromo isophthalic acid and TIB = 1,3,5-tris(imidazol-1-ylmethyl)benzene;[14] [Zn(μ_2-1H-ade)(μ_2-SO_4)]: HAde = 6-Aminopurine/adenine;[15] Yb-MOFs: Yb^{3+} + H_2TCPP;[16] Y-MOF:Eu = $[Y_{0.9}Eu_{0.1}(OBA)(Ox)_{0.5}(H_2O)_2]$, and Tb-MOF:Tb = $[Y_{0.9}Tb_{0.1}(OBA)(Ox)_{0.5}(H_2O)_2]$, (OBA = 4,4′-Oxybis(benzoic acid), Ox = Oxalate);[17] $[Zn(pzt)_2]_n$: Hpzt = 5-(3-pyridyl)-1,3,4-oxadiazole-2-thiol;[18]

[Zn(PAM)(en)]: PAM = 4,4'-methylenebis(3-hydroxy-2-naphthalenecarboxylate), en = 1,2-ethanediamine;[19] $\{[Zn(L)(H_2O)_2]\cdot H_2O\}_n$: H_2L = 5-(4-pyridylamino)isophthalic acid;[21] $\{Cd(INA)(pytpy)(OH)\cdot 2H_2O\}_n$: pytpy = 4'-(4-Pyridinyl)-2,2':6',2"-terpyridine, INA = Isonicotinic acid;[22] $[Cd_3(NTB)_2(DMA)_3]\cdot 2DMA$: H_3NTB = 4,4',4"-nitrilotrisbenzoic acid; DMA = N,N-dimethylacetamide;[23] $\{[Cu^{I}_2(ttpa)_2][Cu^{II}(bptc)]\cdot 3H_2O\cdot DMF\}_n$: ttpa = tris(4-(1,2,4-triazol-1-yl)phenyl)amine, H_4bptc = 3,3',4,4'-biphenyltetracarboxylic acid;[24] $\{[Cu(L)(I)]\cdot(DMF)\cdot H_2O\}_n$: L = 4'-(anthracen-9-yl)-4,2':6',4"-terpyridine;[25] $\{Zn_2(tphn)(2,6\text{-}NDC)_2\cdot 4H_2O\}_n$: tphn = N,N',N'',N'''-tetrakis(2-pyridylmethyl)-1,6-diaminohexane, and 2,6-H_2NDC = 2,6-naphthalenedicarboxylic acid;[26] Zn-NDC-M I: NDC^{2-} = 2,6-naphthalenedicarboxylate and MI = 2-methylimidazole;[27] $[Zn(HL)\cdot 1.5H_2O]$: H_3L = 4-(2,4,6-tricarboxylphenyl)-3,2',6',4''-terpyridine;[28] $\{[Dy(\mu_2\text{-}FcDCA)_{1.5}(MeOH)(H_2O)]\cdot 0.5H_2O\}_n$: FcDCA = 1,1'-ferrocene dicarboxylic acid;[29] $[Zn(ttb)(bdc)_{0.5}]_n$: Httb = 1-(triazo-1-ly)-4-(tetrazol-5-ylmethyl)benzene, H_2bdc = 1,4-benzenedicarboxylic acid;[30] DTZ-COF is synthesized by the condensation of one flexible 2,4,6-tris(4-formylphenoxy)-1,3,5-triazine (TPOT-CHO) unit and one rigid 2,4,6-tris(4-aminophenyl)-1,3,5-triazine (TPT-NH_2) unit;[31] $[Cd_2(H_2L)_2(2,2'\text{-bipy})_2]$ and $[Cd(L)_{0.5}(phen)\cdot 0.5H_2O]$ are constructed using ethylene glycol ether bridging tetracarboxylate ligand 5,5'(4,4'-phenylenebis(methyleneoxy)) diisophthalic acid;[32] $[CuI(BPDPE)]_n$: BPDPE = 4,4'- bis(pyridy)diphenyl ether[33]; $[L_4Cd_3(H_2O)_2]_n$: H_2L = 1,3-(bis(6-(2-methyl)nicotinyl))benzene[34]; $\{Cd(L_2\}_n$: L = 2-(4-(3,5-dicarboxylphenoxy)phenyl) benzimidazole-5-carboylic acid;[35] $\{[WS_4Cu_4I_4[Ni(PBPP)_2]]2DMF]\}_n$: PBPP = 4-phenyl-2,6-bis(20-pyrazinyl)pyridine;[36] $[Eu_2(ppda)_2(npdc)(H_2O)]\cdot H_2O$: H_2ppda = 4-(pyridin-3-yloxy)-phthalic acid and H_2npdc = naphthalene-1,4-dicarboxylic acid.[37]

Table S2. HOMO and LUMO energies calculated for selected nitroaromatic compounds used at B3LYP/6-31G* level.

Analytes	HUMO (eV)	LUMO (eV)	Band Gap (eV)
TNP	-8.24	-3.90	4.34
TNT	-8.46	-3.49	4.97
p-DNB	-8.35	-3.49	4.86
m-DNB	-8.41	-3.13	5.28
BC[38]	-6.56	-2.44	4.12
NB	-7.59	-2.43	5.16
CB[38]	-6.10	-1.45	4.65
PHL[38]	-5.49	-1.10	4.39
DNP	-7.68	-2.83	4.85
p-NP	-6.92	-2.22	4.7
o-NP	-6.91	-2.01	4.9

Reference

1 J. Troyano, J. Perles, P. Amo-Ochoa, J. Ignacio Martínez, M. C. Gimeno, V. Fernández-Moreira, F. Zamora and S. Delgado, *Chem. Eur. J.* 2016, **22**, 1.

2 H. Yu, Q. Liu, M. Fan, J. Sun, Z. Su,X. Li and X. Wang, *Dyes Pigments*, 2020, **197**, 109812.

3 M. Wu, H. Zhang, C. Ge, J. Wu, , S. Ma, Y. Yuan, L. Zhao, T. Yao, X. Zhang and Q. Yang, *Spectrochim. Acta A*, 2022, **264**, 120276.

4 J. Zhang, B. Xu,, F. Luo, G. Tang and C. Zhang, *Polyhedron*, **2019**, 169, 51.

5 B. Xu, F. Luo, G. Tang and J. Zhang, *Acta Cryst.*, 2019, **C75**, 508.

6 B. Dutta, A. Hazra, A. Dey, C. Sinha, P. P. Ray, P. Banerjee, and M. H. Mir, *Cryst. Growth Des.*, 2020, **20**, 765.

7 Y. Yang, X. Song, C. Xu, Y. Wang, G. Zhang and W. Liu, *Dalton Trans.*, 2018, **47**, 11077.

8 J. Zhang, J. Wu, L. Gong, J. Feng and C. Zhang, *ChemistrySelect*, 2017, **2**, 7465.

9 G. Das, B. P. Biswal, S. Kandambeth, V. Venkatesh, G. Kaur, M. Addicoat, T. Heine, S. Verma and R. Banerjee, *Chem. Sci.*, 2015, **6**, 3931.

10 Y. Deng, N. Chen, Q. Li, X. Wu, X. Huang, Z. Lin and Y. Zhao, *Cryst. Growth Des.* 2017, **17**, 3170.

11 T. Geng, D. Li, Z. Zhu, Y. Guan and Y. Wang, *Micropor. Mesopor. Mat.*, 2016, **231**, 92.

12 H. He, S. Chen, D. Zhang, E. Yang and X. Zhao, *RSC Adv.*, 2017, **7**, 38871.

13 J. Li, *J. Mol. Struct.*, 2019, **1**, 160.

14 Y. Rachuri, B. Parmar, K. K. Bisht and E. Suresh, *Dalton Trans.*, 2016, **45**, 7881.

15 Y. Rachuri, B. Parmar, K. K. Bisht and E. Suresh, *Cryst. Growth Des.*, 2017, **17**, 1363.

16 X. Wang, S. Xiao, Z, Jiangm S. Zhen, C. Huang, Q. Liu and Y. Li, *Talanta*, 2021, **234**, 122625.

17 D. Singha, P. Majee, S. Mondal and P. Mahata, *RSC Adv.*, 2015, **5**, 102076.

18 S. Tunsrichon, J. Boonmak and S. Youngme, *Cryst. Growth Des.*, 2019, **19**, 2139.

19 J. Ye, X. Wang, R. F. Bogale, L. Zhao, H. Cheng, W. Gong, J. Zhao and G. Ning, *Sensor Actuat. B,* 2015, **210**, 566.

20 X. Yin, S. Meng and J. Xie, *Polyhedron*, 2018, **139**, 262.

21 A. Zhou, H. Wei, W. Gao, J. Liu and X. Zhang, *CrystEngComm*, 2019, **21**, 5185.

22 J. Zhang, J. Wu, G. Tang, J. Feng, F. Luo, B. Xu and C. Zhang, *Sensor Actuat. B,* 2018, **271**, 166.

23 X. Hu, F. Liu, C. Qin, K. Shao and Z. Su, *Dalton Trans.*, 2015, **44**, 7822.

24 L. Qian, Z. Wang, J. Ding, H. Tian, K. Li, B. Li, H. Li, *Dyes Pigment*s, 2020, **175**, 108159.

25 A. Santra, M. Francis, S. Parshamoni, S. Konar, *ChemistrySelect*, 2017, **2**, 3200.

26 G. Chakraborty and . K. Mandal, *Inorg. Chem.*, 2017, **56**, 14556.

27 T. Kumar, M. Venkateswarulu, B. Das,c A. Halder and R. R. Koner, *Dalton Trans.*, 2019,**48**, 12382.

28 J. Wang, L. Lu, Q. Ding, S. Zhang, J. Wang, A. Singh, A. Kumar and A. Ma, *J. Coord. Chem.*, 2020, **73**, 307.

29 R. Rajak, M. Saraf, S. K. Verma, R. Kumar and S. M. Mobin, *Inorg. Chem.*, 2019, **58**, 16065.

30 S. Gai, R. Fan, J. Zhang, J. Sun, P. Li, Z. Geng, X. Jiang, Y. Dong, J. Wang and Y. Yang, *Inorg. Chem.*, 2021, **60**, 10387.

31 Y. Li, Y. Han, M. Chen, Y. Feng and B. Zhang, *RSC Adv.*, 2019, **9**, 30937.

32 J. Wang, J. Wu, L. Lu, A. Ma, W. Hu, W. Wu, Y. Wu, Y. Sun, A. Singh and A. Kumar, *Polymers*, 2018, **10**, 274.

33 K. Wua, J. Hu, X. Cheng, J. Lia and C. Zhou, *J. Lumin.*, 2020, **219**, 116908.

34 K. Wu, J. Hu, S. Shi, J. Li and X. Cheng. *Dyes Pigment*s, 2020, **173**, 107993.

35 S. Wu, L. Zou, W. Wu, W. Zhong, Y. Wu, X. Liang, L. Li, Y. Wu, Inorg. *Chem. Comm*., 2020, **121**, 108233.

36 Q. Xiang, Q. Qiu, C. Zhang and J. Zhang, *J Clust Sci*., 2021.

37 Z. Zhan, X. Liang, X. Zhang, Y. Jia and M. Hu, *Dalton Trans*., 2019, **48**, 1786.

38 B. Wang, X. Lv, D. Feng, L. Xie, J. Zhang, M. Li, Y. Xie, J. Li and H. Zhou, *J. Am. Chem. Soc.*, 2016, **138**, 6204.